RSC Advances

ROYAL SOCIETY OF CHEMISTRY

www.rsc.org/advances

Journal Name

COMMUNICATION

Fabrication of Fe_3O_4@SiO_2@RGO nanocomposites and their excellent absorption properties with low filler content

Ya-Fei Pan, Guang-Sheng Wang*, Yong-Hai Yue*

Received 00th January 20xx,

Accepted 00th January 20xx

DOI: 10.1039/x0xx00000x

www.rsc.org/

Novel Fe_3O_4@SiO_2@RGO nanocomposites were fabricated and the nanocomposites which were embedded into paraffin wax with low filler content (20 wt%) showed excellent microwave absorption properties. The minimum reflection loss can reach -26.6 dB at 9.7 GHz, and the reflection loss was less than -10 dB in the frequency range from 4.4 to 17.3 GHz with an absorber thickness of 2.0-5.0 mm. Compared with the pure Fe_3O_4 and Fe_3O_4@SiO_2, the Fe_3O_4@SiO_2@RGO nanocomposites exhibited superior absorption properties. The mechanism of enhanced wave absorption properties was explained.

Introduction

In recent years, with the fast development of wireless communication and the extensive utilization of electronic devices, electromagnetic interference has become a new environmental problem. Hence, much attention has focused on high-performance microwave absorption materials, which have prospective applications in reduction of electromagnetic radiation and improvement of electromagnetic interference shielding.[1-3] Over the past decades, due to the strong absorption and large anisotropic energy, ferrites have attracted considerable attention to develop novel microwave absorption materials.[4-6] Among the various ferrite materials, extensive studies have been done to develop the magnetite (Fe_3O_4) as microwave absorber, with the advantages of low cost and strong absorption.[7]

As a typical double-complex medium with dielectric loss and magnetic loss, Fe_3O_4 filled as absorber can exhibit good microwave absorption property, which has been reported by S. Kolev et al. [8] The minimum calculated reflection loss can reach -25 dB at 6.9 GHz with 35 wt% Fe_3O_4 when the matching thickness is 4 mm. Ni et al. [9] prepared well-dispersed Fe_3O_4 nanocrystals and obtained the minimum reflection loss value of -21.2 dB at 8.2 GHz at the 30 wt% filler content. Wei et al. [10] studied the microwave absorption properties of Fe_3O_4 magnetic films and the results showed that the matching frequency for reflection loss exceeded -20 dB at 13.0 GHz. Many researchers have concentrated on improving the microwave absorption performance, for example considering the impedance matching problem, the Fe_3O_4 nanocomposites with core-shell or yolk-shell structure, including Fe_3O_4@SnO_2,[11] Fe_3O_4@TiO_2,[12] Fe_3O_4@ZnO,[13] have been reported. However, as an important microwave absorber, Fe_3O_4 particles show some shortcomings: such as narrow absorption frequency, high filler content, poor environmental stability; while, narrow absorption frequency, the high density and poor environmental stability of these nanocomposites will restrict the wide application as excellent microwave absorber which should exhibit the advantages of strong absorption, wide absorption frequency, lightweight, and high stability.[14, 15] Furthermore, coating magnetic nanomaterials with an insulting material is realized as an effective way to increase the surface anisotropic energy and prevent the core materials from oxidation. In the case of silica-coated iron oxide, the coating materials can also disperse on the surface more uniformly owing to the existence of hydroxyl groups, in addition, a better match of the dielectric loss and magnetic loss may be realized by the existence of the protective silica shell.[16]

At the meantime, compared with traditional microwave absorption materials, reduced graphene oxide (RGO) has been applied as a new wave absorption material because of its desirable physical and chemical properties.[17, 18] Recently, Wang et al. reported a series of materials coated by RGO sheets which showed enhanced microwave absorption.[6, 19-21] Generally, the enhanced microwave absorption of these RGO-based materials may mainly arise from large aspect ratio, high conductivity and residual defects on the surface of the RGO sheets,[22, 23] which cause electronic dipole polarization and interfacial polarization.

In this paper, we introduce the synthesized Fe_3O_4 magnetic nanoparticle clusters with relatively uniform sizes by hydrothermal reaction. The chemical stability of magnetic nanoparticle clusters was improved by silica coating. Moreover, Fe_3O_4@SiO_2@RGO nanocomposites were synthesized under ultrasonic treatment, and their wave absorption properties and the mechanism of enhanced wave absorption properties were also studied.

Experimental section

Materials

Ferric chloride hexahydrate ($FeCl_3 \cdot 6H_2O$), anhydrous sodium acetate, ethylene glycol(EG), ethylenediaminetetraacetic acid disodium salt (EDTA-2Na), tetraethyl orthosilicate (TEOS, 98 wt%), ammonia solution (28 wt%), and anhydrous ethanol were all purchased from Alfa Aesar. All chemicals were of analytical reagent grade and were used as received.

Preparation of Fe_3O_4 magnetic nanoparticle clusters (MNCs)

In the synthesis process of about 200nm MNCs, $FeCl_3 \cdot 6H_2O$ (2.028 g), NaAc (3.69 g), and EDTA-2Na (0.023 g) were dissolved in ethylene glycol (60 mL) under stirring. Then ultrasonic treatment for 20 min, the obtained homogeneous dark yellow solution was transferred to a Teflon-lined stainless-steel autoclave and heated at

200 °C for 10 h and then naturally cooled down to room temperature. After that, the dark precipitates were washed with water and ethanol three times each other, and then dried in vacuum for 24 h.

Preparation of Fe_3O_4@SiO_2 microspheres

For silica coating, the core-shell Fe_3O_4@SiO_2 microspheres were synthesized through a modified Stöber method. Typically, 0.0258 g of the as-prepared Fe_3O_4 MNCs were dispersed in a mixture of ethanol (40 mL), water (6 mL), and ammonia solution (1 mL). Briefly, TEOS (0.17 mL) was added into the above dispersion and the reaction was allowed to proceed for 1 h under stirring and ultrasonic treatment. Then the product was collected with the help of magnet and washed three times with ethanol and water, and dried at 60 °C for 8 h under vacuum.

Preparation of Fe_3O_4@SiO_2@RGO nanocomposites

Typically, graphite oxide (GO) was synthesized by a modified Hummers method.[24] The RGO synthesis process was the same with Wang and his co-workers previously reported.[25] To get the nanocomposites, 30 mg of Fe_3O_4@SiO_2 microspheres was added to RGO suspension and sonicated for 2 h. Afterwards, the product was isolated by centrifugation and washed with ethanol, and finally freeze-dried.

Characterization

The samples XRD data were measured using X-ray diffractometer (D/MAX-1200, Rigaku Denki Co. Ltd, Japan) with Cu Ka radiation at λ=0.15406nm. To observe the morphology, size and microstructure of the nanocomposites, scanning electron microscopy (SEM, JSM-7500F) and transmission electron microscopy (TEM, JEOL-2100F) were used. The lakeshore vibrating sample magnetometer (VSM, Riken Denshi Co. Ltd, Japan) was used to measure the magnetic properties of the samples at room temperature.

Microwave absorption performance measurement

The composites used for EM absorption measurement were prepared by mixing the products with paraffin wax in different mass percentages and pressed into a cylindrical shaped compact (Φ_{out}=7.00 mm and Φ_{in}=3.04 mm). The EM parameters of the composites were measured by the transmission/reflection coaxial line method. And the values of complex permittivity and permeability were measured in the 2-18 GHz frequency range by an Aligent N5244a net work analyzer.

Results and discussion

As shown in Figure 1a, the Fe_3O_4 MNCs display monodispersed characteristic with the diameter in the range of 180-220 nm. It can be observed that the as-prepared MNCs with rough surface suggested such secondary structure was built up by subunit grains. Figure 1b shows a high-resolution TEM image of the individual Fe_3O_4 MNC. It can be clearly seen that regularly paralleled lattice fringes with the space between neighboring lattices is about 0.29 nm, which indicates the single-crystal nature of the specific subunit nanocrystals.[26] From Figure 1c, it indicates that the core-shell structure of the Fe_3O_4@SiO_2 microspheres. It is visible that the smooth surface and a uniform SiO_2 layer encapsulates the Fe_3O_4 MNC. And the insert of figures indicate the thickness of SiO_2 is about 30 nm. Moreover, Figure 1d provides a representative image of the Fe_3O_4@SiO_2@RGO nanocomposites, and the Figure S1 shows the FESEM image of the Fe_3O_4@SiO_2@RGO nanocomposites and corresponding elemental maps of Fe, Si, O and C, it can confirm that the Fe_3O_4@SiO_2 nanoparticles were coated by RGO absolutely.

To confirm the phases and structures of the as-prepared samples, the XRD of Fe_3O_4, Fe_3O_4@SiO_2, and Fe_3O_4@SiO_2@RGO were shown in the Figure 2a. From the XRD pattern of Fe_3O_4 MNCs, it can be observed that all the diffraction peaks are readily indexed to the face-centered cubic structure of Fe_3O_4 (JCPDS NO. 88-0315). The narrow sharp peaks mean that the Fe_3O_4 magnetic nanoparticle clusters are highly crystallized. Moreover, the lower XRD pattern of Fe_3O_4@SiO_2 is almost same as that Fe_3O_4 MNCs. Therefore, no peaks from SiO_2 can be confirmed implying that formed SiO_2 shell is amorphous phase. In addition, the absence of X-ray diffraction sharp peak for graphite at around 26° suggests that the RGO nanosheets disperse on the surface of Fe_3O_4@SiO_2 microspheres homogeneously.[27, 28] The electronic structure of graphite and graphene-based materials can be analysed by Raman spectroscopy. Figure 2b represents the Raman spectra of GO and Fe_3O_4@SiO_2@RGO nanocomposites. It can be observed that there are no obvious changes of the positions and shapes of the D band and G band of RGO in the nanocomposites, compared with GO. The intensity ratio of I_D/I_G is used to evaluate the ordered and disordered crystal structures of carbon.[29] The I_D/I_G ratio is 1.14 for GO, and 1.43 for the composites. The change in I_D/I_G ratio explains the fact that the reduction of GO leads to smaller but more numerous sp^2 domains in the carbon.[30]

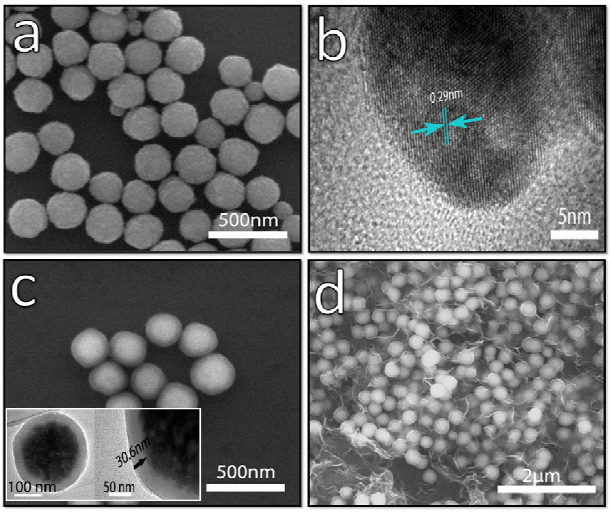

Figure 1. (a) SEM image overview of the as-prepared Fe_3O_4 magnetic nanoparticle clusters; (b) HRTEM image of Fe_3O_4 MNC; (c) SEM image of Fe_3O_4@SiO_2 microspheres and TEM images (insert) of Fe_3O_4@SiO_2; (d) SEM image of Fe_3O_4@SiO_2@RGO nanocomposites

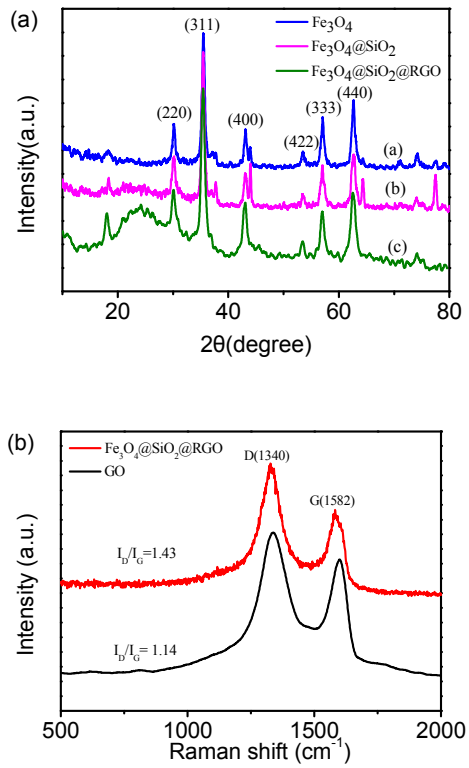

Figure 2. (a) XRD patterns of Fe_3O_4 magnetic nanoparticle clusters, Fe_3O_4@SiO_2 microspheres and Fe_3O_4@SiO_2@RGO nanocomposites; (b) Raman spectra of GO and Fe_3O_4@SiO_2@RGO.

The magnetization of the as-prepared various samples were measured at room temperature, and presented in Fig 3. The saturation magnetization (*Ms*) and coercivity (*Hc*) values were shown at Table1. The *Ms* of the Fe_3O_4@SiO_2 and Fe_3O_4@SiO_2@RGO decrease due to the presence of the SiO_2 and RGO coating, however, the *Hc* values instead increase suggesting the larger anisotropic energy. In addition, these three kinds of samples express typical ferromagnetic behavior.

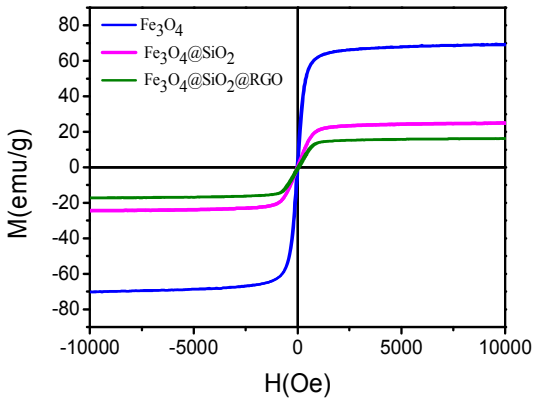

Figure 3. Magnetization hysteresis loops of the Fe_3O_4 MNCs, Fe_3O_4@SiO_2 microspheres, and Fe_3O_4@SiO_2@RGO nanocomposites measured at room temperature.

Table 1. Magnetic properties of the products

Sample	M_s((emu/g)	H_c (Oe)
Fe_3O_4	70.3	30.2
Fe_3O_4@SiO_2	25.1	45.1
Fe_3O_4@SiO_2@RGO	17.1	55.6

Owing to the special structure, the samples may have good microwave absorption properties. Therefore, to test microwave absorption performance, various contents of samples mixed with paraffin wax to synthesize composites in a press process. Based on the measured data of permittivity and permeability, the reflection loss (RL) values can be calculated by the following expression:[31, 32]

$$Z_{in} = \sqrt{\frac{\mu_r}{\varepsilon_r}} \tanh\left[j\left(\frac{2f\pi d}{c}\right)\sqrt{\mu_r \varepsilon_r}\right] \quad (1)$$

$$R = 20\log\left|\frac{Z_{in}-1}{Z_{in}+1}\right| \quad (2)$$

where Z_{in} is the normalized input characteristic impedance; ε_r ($\varepsilon_r=\varepsilon'-j\varepsilon''$) and μ_r ($\mu_r=\mu'-j\mu''$) are the complex permittivity and permeability of absorber; f is the frequency; d is the thickness of the absorber, and c is the velocity of light in free space.

It can be observed that the Fe_3O_4@SiO_2@RGO+wax composites exhibit enhanced wave absorption properties. Figure 4a shows the theoretical reflection loss (RLs) of composites 20 wt% Fe_3O_4, 10 wt% Fe_3O_4@SiO_2, 20 wt% Fe_3O_4@SiO_2, 10 wt% Fe_3O_4@SiO_2@RGO and 20 wt% Fe_3O_4@SiO_2@RGO, with paraffin wax at a thickness of 3.0 mm. It shows that the RLs of Fe_3O_4@SiO_2@RGO+wax composites are much higher than other composites, especially at a filler content of only 20 wt%. The minimum reflection loss of the composites reaches -26.6 dB at 9.7 GHz, and the frequency bandwidth less than -10 dB is from 8.4 to 11.8 GHz. Moreover, at the filler content of 10 wt%, the RLs can reach 15.4 dB at 11.4 GHz, and the frequency bandwidth less than -10 dB is from 11.1 to 14.1 GHz. Figure 4b shows the calculated theoretical RLs of Fe_3O_4@SiO_2@RGO+wax composites at various thicknesses (2-5 mm) with the filler loading of 20 wt%. It indicates that the microwave absorbing properties and the minimum RLs corresponding to the maximum absorptions gradually appeared in different frequency can be tunable by controlling the thickness of the absorbers. And it worth noted that the materials attained a reflection loss of less than -10 dB in the frequency range from 4.4 to 17.3 GHz with an absorber thickness of 2.0-5.0 mm, confirming that this kind of composite is a broadband wave-absorbing material, which is quite beneficial to many electromagnetic shielding material designed to reduce electromagnetic waves over a wide frequency range.[33, 34] With the lower filler content, the composites can have strong absorption and wide absorption frequency, compared with other Fe_3O_4-based materials reported as microwave absorber.[9, 14] To demonstrate the Fe_3O_4@SiO_2@RGO nanocomposites greatly enhanced the wave absorption properties, for comparison, the three-dimensional presentations of RLs were also shown in Figure 4c and 4d, the images displayed the RLs of Fe_3O_4@SiO_2@RGO+wax and Fe_3O_4@SiO_2+wax with different thicknesses in the range of 2-18

GHz with the same loading. Except for the enhanced wave absorption properties, the Fe_3O_4@SiO_2@RGO+wax materials are still as flexible and can be made into different shapes.

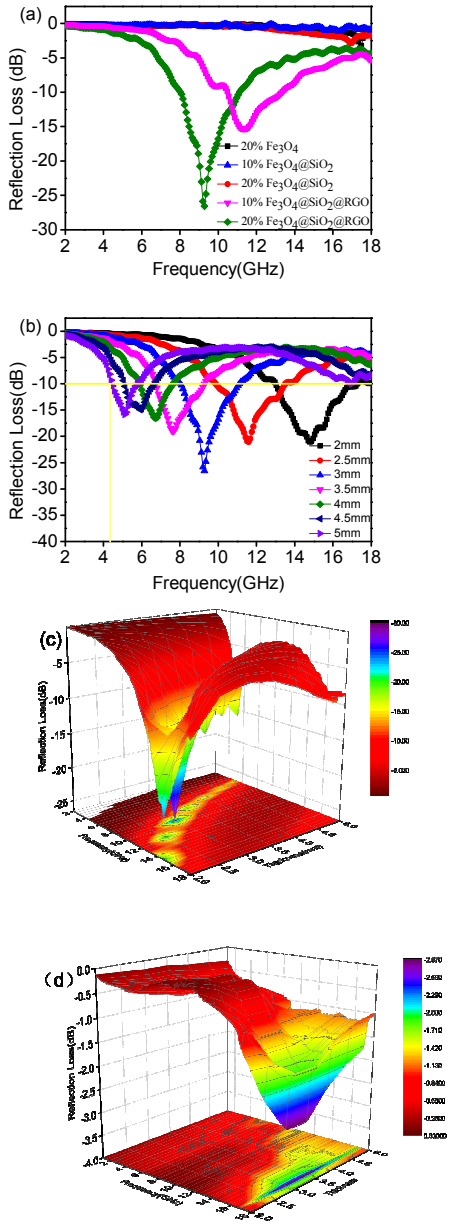

Figure 4. Reflection losses of (a) the products with a thickness of 3.0 mm in the range of 2-18 GHz; (b) the 20 wt% filler content of Fe_3O_4@SiO_2@RGO+wax composites with thickness 2-5 mm. Three-dimensional presentations of the reflection losses of the 20 wt% filler content of (c) Fe_3O_4@SiO_2@RGO+wax composites; (d) Fe_3O_4@SiO_2+wax composites.

To investigate the possible electromagnetic wave absorption mechanism of samples, the frequency dependence relative permittivity and permeability for materials are displayed in Figure 5. The real permittivity and permeability are connected with the storage ability of electromagnetic energy, whereas the imaginary permittivity and permeability are linked with energy dissipation and magnetic loss.[35] It can be seen that the values of ε' and ε" for Fe_3O_4@SiO_2@RGO+wax composites are much larger than pure Fe_3O_4+wax and Fe_3O_4@SiO_2+wax, which indicates that RGO can greatly improve the dielectric properties of composites. The ε' values of 20 wt% Fe_3O_4@SiO_2@RGO+wax are in the range of 6.7-9.2, which is slightly larger than 10 wt% Fe_3O_4@SiO_2@RGO+wax , while the ε" values vary from 1.9-2.5, suggesting the strong dielectric loss in almost all frequency region. Moreover, the variation tendency of μ' and μ" for these composites are basically the same, especially the negative μ" values appear in composites, which signifies the magnetic energy radiate out without any absorption.[36]

It can be concluded that the values of dielectric tangent loss are higher than magnetic tangent loss for Fe_3O_4@SiO_2@RGO composites from Figure S2, which means that the main loss mechanism is dielectric loss rather than magnetic loss. The maximum value of dielectric tangent loss is 0.37 (9.7 GHz), which is accordance with the reflection loss peak (shown in Figure 4a). We need to emphasize that the dielectric loss values are improved dramatically and the magnetic loss values almost have no change after combining with RGO. The causes for dielectric loss include electronic dipole polarization and interfacial polarization.[37-39] Firstly, electrons in Fe_3O_4 can transfer between Fe^{2+} and Fe^{3+} ions as EM wave applied, producing dipole polarization in the composites, which has significant effects on the dielectric loss. Moreover, interface polarization arises when the neighboring phases differ from each other in a dielectric constant, conductivity, or both at measuring frequencies. For Fe_3O_4@SiO_2@RGO composites, the interface mainly caused by RGO, so that verifies RGO reported as before is beneficial to EM absorption properties.[22, 32, 40]

According to Van Der Zaag's research achievement,[41] for magnetic materials, the magnetic loss mainly derives from eddy current effect, hysteresis, natural resonance, and domain wall resonance.[42] However, the hysteresis loss is negligible in the weak field, and the domain wall resonance loss commonly occurs at MHz frequency.[43] Therefore, the eddy current effect and natural resonance may be responsible for the attenuation of EM waves over 2-18 GHz frequency range. The eddy current loss can be calculated by the following equation:

$$\mu'' \approx 2\pi\mu_0(\mu')^2\sigma \cdot d^2 f/3 \quad (3)$$

Where μ_0 $(H \cdot m^{-1})$ and σ $(S \cdot cm^{-1})$ are the electric permeability and the conductivity in vacuum, respectively. If the reflection loss is caused by eddy current loss effect, the values of C_0 $(C_0=\mu''(\mu')^{-2}f^{-1})$ are constant when the frequency varies. From figure 6, it can be observed that the value of C_0 is almost constant with the frequency range from 6-17 GHz, which suggests that the composites have an obvious eddy current effect for the microwave energy dissipation.

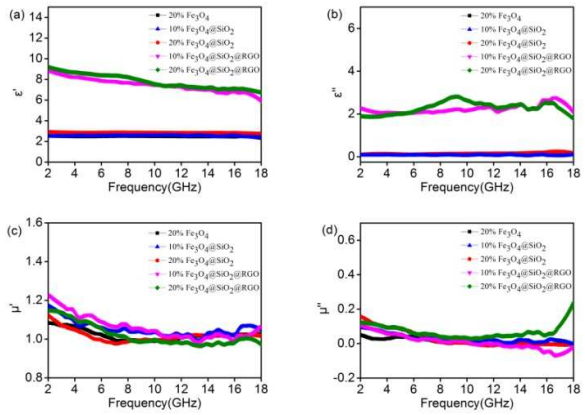

Figure 5. (a) real and (b) imaginary parts of relative complex permittivity; (c) real and imaginary parts of relative complex permeability for paraffin wax composites in the frequency range of 2-18 GHz.

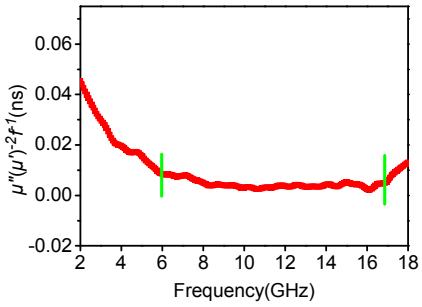

Figure 6. The C_0-f curve of 20 wt% Fe_3O_4@SiO_2@RGO+wax composites

Another mechanism for magnetic loss is natural resonance, which can be expressed in the following equation:[44]

$$2\pi f_r = rHa \quad (4)$$

$$Ha = 4|K_1|/3\mu_0 Ms \quad (5)$$

where r is the gyromagnetic ratio, Ha is the anisotropy energy, and $|K_1|$ is the anisotropy coefficient, Ms is the saturation magnetization. The resonance frequency depends on the effective anisotropy field, which is associated with coercivity value of the materials.[38, 45] As shown in Table 1, the coercivity value of Fe_3O_4@SiO_2@RGO nanocomposites is highest among the various materials, which is also beneficial to EM wave absorption.

Conclusions

In summary, the Fe_3O_4@SiO_2@RGO nanocomposites with an obviously enhanced microwave absorption property have been successfully synthesized by combining the versatile sol-gel process with hydrothermal reaction. The nanocomposites (at filler content of only 20 wt%) exhibits excellent microwave absorption properties in terms of both the minimum reflection loss value and the absorption bandwidth over 2-18 GHz. The minimum reflection loss can reach -26.6 dB at 9.7 GHz with the thickness of 3.0 mm, and the absorption bandwidth with a reflection loss below -10 dB up to 12.9 GHz (4.4-17.3 GHz). Therefore, it is believed that the Fe_3O_4@SiO_2@RGO nanocomposites are good candidate for microwave absorption absorbers with strong absorption, wide absorption frequency, lightweight, which are promising for applications in military and commercial fields.

Acknowledgements

This project was supported by the National Natural Science Foundation of China (No. 51472012), and the Fundamental Research Funds for the Central Universities.

Key Laboratory of Bio-Inspired Smart Interfacial Science and Technology of Ministry of Education, School of Chemistry and Environment, Beihang University, Beijing 100191, PR China. Correspondence should be addressed to Guang-Sheng Wang,

E-mail: wanggsh@buaa.edu.cn

† Footnotes relating to the title and/or authors should appear here. Electronic Supplementary Information (ESI) available: [details of any supplementary information available should be included here]. See DOI: 10.1039/x0xx00000x

Notes and references

1. W. Zhu, L. Wang, R. Zhao, J. Ren, G. Lu and Y. Wang, *Nanoscale*, 2011, **3**, 2862-2864.
2. J. Xu, J. Liu, R. Che, C. Liang, M. Cao, Y. Li and Z. Liu, *Nanoscale*, 2014, **6**, 5782-5790.
3. X.-M. Meng, X.-J. Zhang, C. Lu, Y.-F. Pan and G.-S. Wang, *J. Mater. Chem. A.*, 2014, **2**, 18725-18730.
4. S. Tyagi, H. B. Baskey, R. C. Agarwala, V. Agarwala and T. C. Shami, *Ceram. Int.*, 2011, **37**, 2631-2641.
5. W. Fu, S. Liu, W. Fan, H. Yang, X. Pang, J. Xu and G. Zou, *J. Magn. Magn. Mater.*, 2007, **316**, 54-58.
6. X.-J. Zhang, G.-S. Wang, W.-Q. Cao, Y.-Z. Wei, J.-F. Liang, L. Guo and M.-S. Cao, *ACS Appl. Mater. Inter.*, 2014, **6**, 7471-7478.
7. J. Zou, Z. Wang, M. Yan and H. Bi, *J. Phys. D: Appl. Phys.*, 2014, **47**, 275001.
8. S. Kolev, A. Yanev and I. Nedkov, *Phys. Status Solidi C.*, 2006, **3**, 1308-1315.
9. S. Ni, S. Lin, Q. Pan, F. Yang, K. Huang and D. He, *J. Phys. D: Appl. Phys.*, 2009, **42**, 055004.
10. J. Wei, J. Liu and S. Li, *J. Magn. Magn. Mater.*, 2007, **312**, 414-417.
11. J. Liu, J. Cheng, R. Che, J. Xu, M. Liu and Z. Liu, *J. Phys. Chem.C*, 2013, **117**, 489-495.
12. J. Liu, R. Che, H. Chen, F. Zhang, F. Xia, Q. Wu and M. Wang, *Small*, 2012, **8**, 1214-1221.
13. D. Sun, Q. Zou, Y. Wang, Y. Wang, W. Jiang and F. Li, *Nanoscale*, 2014, **6**, 6557-6562.
14. X. Liu, Y. Chen, X. Cui, M. Zeng, R. Yu and G.-S. Wang, *J. Mater. Chem. A.*, 2015, **3**, 12197-12204.
15. X. Li, B. Zhang, C. Ju, X. Han, Y. Du and P. Xu, *J. Phys. Chem. C*, 2011, **115**, 12350-12357.
16. H. Hekmatara, M. Seifi, K. Forooraghi and S. Mirzaee, *PCCP*, 2014, **16**, 24069-24075.

17. A. K. Geim, *Science*, 2009, **324**, 1530-1534.
18. M. J. Allen, V. C. Tung and R. B. Kaner, *Chem. Rev.*, 2010, **110**, 132-145.
19. X.-J. Zhang, G.-S. Wang, Y.-Z. Wei, L. Guo and M.-S. Cao, *J. Mater. Chem. A.*, 2013, **1**, 12115-12122.
20. D. Chen, G.-S. Wang, S. He, J. Liu, L. Guo and M.-S. Cao, *J. Mater. Chem. A.*, 2013, **1**, 5996-6003.
21. X.-J. Zhang, G.-S. Wang, W.-Q. Cao, Y.-Z. Wei, M.-S. Cao and L. Guo, *RSC Adv.*, 2014, **4**, 19594-19601.
22. C. Wang, X. Han, P. Xu, X. Zhang, Y. Du, S. Hu, J. Wang and X. Wang, *Appl. Phys. Lett.*, 2011, **98**, 072906.
23. J. Liang, Y. Wang, Y. Huang, Y. Ma, Z. Liu, J. Cai, C. Zhang, H. Gao and Y. Chen, *Carbon*, 2009, **47**, 922-925.
24. W. S. Hummers and R. E. Offeman, *J. Am. Chem. Soc.*, 1958, **80**, 1339-1339.
25. G.-S. Wang, Y. Wu, Y.-Z. Wei, X.-J. Zhang, Y. Li, L.-D. Li, B. Wen, P.-G. Yin, L. Guo and M.-S. Cao, *ChemPlusChem*, 2014, **79**, 375-381.
26. M. Lin, H. Huang, Z. Liu, Y. Liu, J. Ge and Y. Fang, *Langmuir*, 2013, **29**, 15433-15441.
27. X. Bai, Y. Zhai and Y. Zhang, *J. Phys. Chem.C*, 2011, **115**, 11673-11677.
28. Y. Wang, R. Cheng, Z. Wen and L. Zhao, *Eur. J. Inorg. Chem.*, 2011, **19**, 2942-2947.
29. M. Zhang, M. Jia and Y. Jin, *Appl. Surf. Sci.*, 2012, **261**, 298-305.
30. J. Su, M. Cao, L. Ren and C. Hu, *J. Phys. Chem. C*, 2011, **115**, 14469-14477.
31. M.-S. Cao, X.-L. Shi, X.-Y. Fang, H.-B. Jin, Z.-L. Hou, W. Zhou and Y.-J. Chen, *Appl. Phys. Lett.*, 2007, **91**, 203110.
32. G.-S. Wang, L.-Z. Nie and S.-H. Yu, *RSC Adv.*, 2012, **2**, 6216-6221.
33. Y. Zhang, Y. Huang, T. Zhang, H. Chang, P. Xiao, H. Chen, Z. Huang and Y. Chen, *Adv. Mater.*, 2015, **27**, 2049-2053.
34. Y. Egami, T. Yamamoto, K. Suzuki, T. Yasuhara, E. Higuchi and H. Inoue, *J. Mater. Sci.*, 2012, **47**, 382-390.
35. W. Zhou, X. Hu, X. Bai, S. Zhou, C. Sun, J. Yan and P. Chen, *ACS Appl. Mater. Inter.*, 2011, **3**, 3839-3845.
36. C. Wang, X. Han, X. Zhang, S. Hu, T. Zhang, J. Wang, Y. Du, X. Wang and P. Xu, *J. Phys. Chem.C*, 2010, **114**, 14826-14830.
37. Y. J. Chen, P. Gao, C. L. Zhu, R. X. Wang, L. J. Wang, M. S. Cao and X. Y. Fang, *J. Appl. Phys.*, 2009, **106**, 054303.
38. Y.-J. Chen, P. Gao, R.-X. Wang, C.-L. Zhu, L.-J. Wang, M.-S. Cao and H.-B. Jin, *J. Phys. Chem. C*, 2009, **113**, 10061-10064.
39. J. Liu, J. Xu, R. Che, H. Chen, Z. Liu and F. Xia, *J. Mater. Chem.*, 2012, **22**, 9277-9284.
40. Y.-Z. Wei, G.-S. Wang, Y. Wu, Y.-H. Yue, J.-T. Wu, C. Lu and L. Guo, *J. Mater. Chem. A.*, 2014, **2**, 5516-5524.
41. P. J. van der Zaag, *J. Magn. Magn. Mater.*, 1999, **196**, 315-319.
42. Y. Du, W. Liu, R. Qiang, Y. Wang, X. Han, J. Ma and P. Xu, *ACS Appl. Mater. Inter.*, 2014, **6**, 12997-13006.
43. M. Wu, Y. D. Zhang, S. Hui, T. D. Xiao, S. Ge, W. A. Hines, J. I. Budnick and G. W. Taylor, *Appl. Phys. Lett.*, 2002, **80**, 4404-4406.
44. C. Kittel, *Physical Review*, 1948, **73**, 155-161.
45. Y.-J. Chen, G. Xiao, T.-S. Wang, Q.-Y. Ouyang, L.-H. Qi, Y. Ma, P. Gao, C.-L. Zhu, M.-S. Cao and H.-B. Jin, *J. Phys. Chem. C*, 2011, **115**, 13603-13608.

Graphical abstract

The Fe_3O_4@SiO_2@RGO nanocomposites with enhanced microwave absorption properties have been fabricated. The results indicate that the minimum reflection loss can reach -26.6 dB at 9.7 GHz with low filler content, and the enhanced mechanism was also explained.

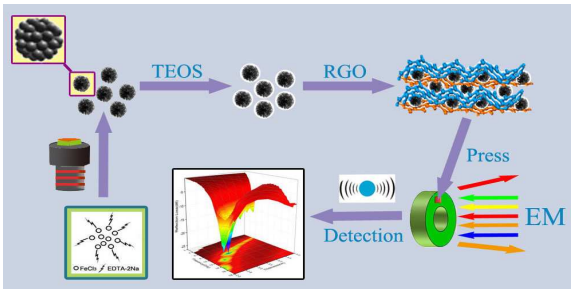

Supporting Information

Fabrication of Fe_3O_4@SiO_2@RGO nanocomposites and their excellent absorption properties with low filler content

Ya-Fei Pan, Guang-Sheng Wang*, Yong-Hai Yue*

Key Laboratory of Bio-Inspired Smart Interfacial Science and Technology of Ministry of Education, School of Chemistry and Environment, Beihang University, Beijing 100191, PR China.

Correspondence should be addressed to Guang-Sheng Wang, E-mail: wanggsh@buaa.edu.cn

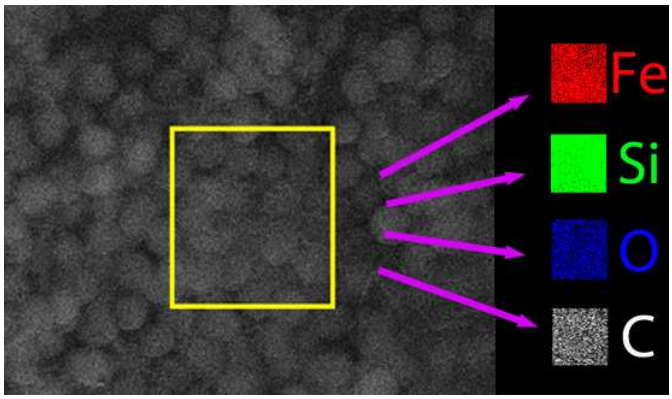

Figure S1. FESEM image of the Fe_3O_4@SiO_2@RGO nanocomposites and corresponding elemental maps of Fe, Si, O and C

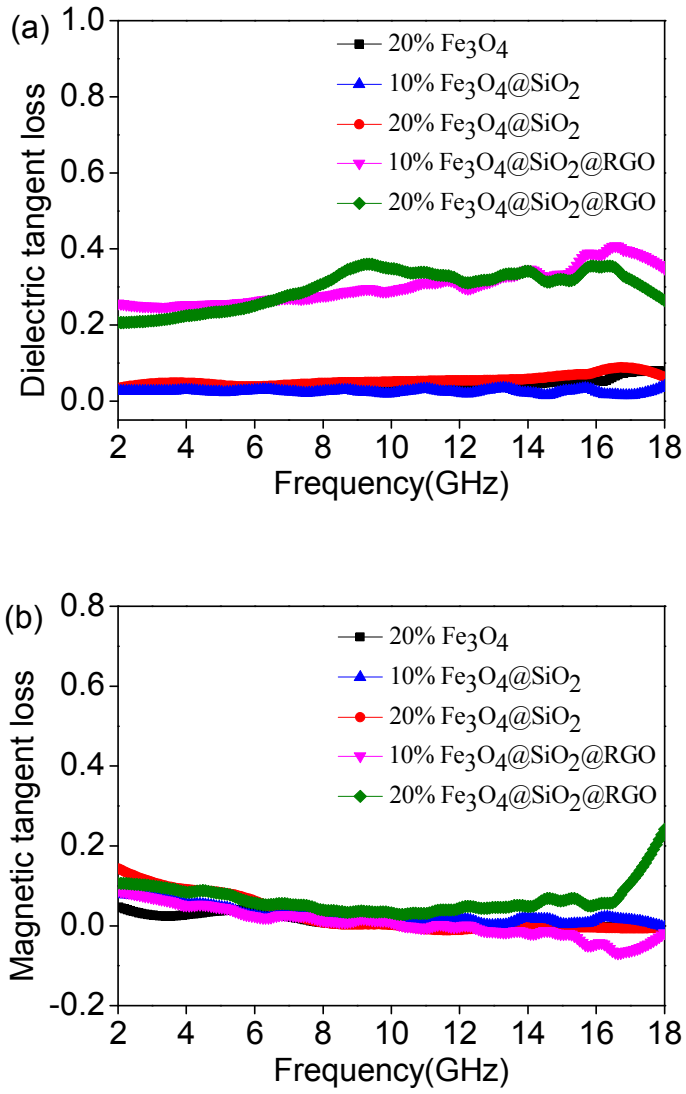

Figure S2. Frequency dependence of (a) dielectric tangent loss and (b) magnetic tangent loss of samples